DOI: 10.1002/ejic.200900807

Mechanistic Information on the Reversible Binding of NO to Mono- and Dinuclear Fe^{II} Complexes of a Biomimetic S_4N Ligand

Shaban Y. Shaban[a,b] and Rudi van Eldik*[a]

Keywords: Biomimetics / Kinetics / Nitrogen oxides / [FeS] core / Nitrogenases

Structural and mechanistic information on the binding of NO to mono- and dinuclear [$Fe^{II}(S_4NNEt_2)$] fragments as potential catalysts for the removal of NO from effluent gas streams have been obtained from concentration, temperature and pressure dependent kinetic measurements using stopped-flow techniques. The results indicate that the steric and electronic structure only affect the rate but not the nature of the binding mechanism by which NO coordinates to the selected complexes. Therefore, the sterically hindered dinuclear complex [$Fe^{II}(S_4NNEt_2)]_2$ binds NO ca. eight times slower than the corresponding mononuclear complex [$Fe^{II}(CH_3OH)(S_4NNEt_2)$]. Significantly negative $\Delta S^{\#}$ values were found for the binding of NO to both the mono- and dinuclear species, and are consistent with an associative mechanism. The negative volumes of activation observed for the binding of NO to both dinuclear [$Fe^{II}(S_4NNEt_2)]_2$ and mononuclear [$Fe^{II}(CO)(S_4NNEt_2)$] complexes further supports the operation of an associative mechanism. Structural studies on the [$Fe^{II}(NO)(S_4NNEt_2)$] complex indicate it to be six-coordinate, low-spin iron(II) with a neutral NO ligand.

Introduction

There exists an ongoing interest in the chemistry of transition metal nitrosyl complexes, especially in their structural and electronic properties, as well as their reactivity. More recently this interest is focused on nitrosyl complexes as potential waste gas purification catalysts,[1] as drugs releasing the neuro-transmitter and mammalian bioregulator NO,[2] or as model complexes for metal enzymes such as nitrile hydratase,[3] cytochrome oxidase,[4] and nitrogenases,[5] and in the use of metallonitrosyl complexes as pharmaceutical reagents.[6] Particularly interesting are also those complexes which can deliver NO to biological targets on demand.[7] In a few cases NO complexes can serve as precursors for N_2 complexes, which are considered to represent the primary species when N_2 binds to the active sites of FeMo, FeVor and FeFe nitrogenases.[5] A great deal of spectroscopic information on NO complexes allows a correlation with the structure and stability of NO complexes.[8]

In the search for low molecular weight compounds that combine structural and reactivity features of [FeS] enzymes, iron complexes containing [$Fe^{II}(S_4NR)$] fragments, where $(S_4NR)^{2-}$ = 2,6-bis(2-mercaptophenylthiomethyl)-4-substituted pyridine(2–), were found to represent a class of synthetic models of nitrogenases as, i) they exhibit a biologically relevant [FeS] core in which two iron centers are bridged via bis(μ-thiolato) donor atoms; ii) they dissociate reversibly in solution to give the mononuclear species and leave a free coordination site suitable for binding and activation of relevant small molecules like NO, NO^+ and CO.[9]

[$Fe^{II}(S_4NR)$] fragments can bind NO (from NO gas) or NO^+ (from $NOBF_4$) to produce the corresponding nitrosyl complexes with the formal binding mode Fe^{II}–$NO^{\cdot}$ or Fe^{II}–NO^+, respectively. The latter complex can be reduced to form the Fe^{II}–$NO^{\cdot}$ complex. The majority of metal nitrosyl complexes have 18 valency electron (VE) configurations. For the elucidation of redox mechanisms, a point of considerable interest is the consequences caused by one-electron reductions of 18 VE nitrosyl complexes to give 19 VE species. 19 VE complexes are usually highly labile and too unstable for isolation and complete characterization, but nitrosyl complexes with [$Fe^{II}(S_4NR)$] cores yielded a few exceptions to this rule. One electron reduction of [$Fe^{II}(NO)(S_4NR)]^+$ gave the labile but isolable 19 VE complexes [$Fe^{II}(NO^{\cdot})(S_4NR)$]. The neutral 19 VE complex [$Fe^{II}(NO^{\cdot})(S_4NR)$] could be isolated in the solid state and completely characterized.[9a]

It is the objective of this study to perform a detailed mechanistic study of the reaction of NO with different [$Fe^{II}(S_4NR)$] fragments in solution in order to reveal the rate and activation parameters for the reversible binding of NO, and to clarify the underlying reaction mechanism. This work provides also an evaluation of the influence of steric and electronic factors of the [$Fe^{II}(L)(S_4NR)$] (L = bridging thiolato σ-donor S atom, CH_3OH, or CO, Scheme 1) frag-

[a] Inorganic Chemistry, Department of Chemistry and Pharmacy, University of Erlangen-Nürnberg,
Egerlandstr. 1, 91058 Erlangen, Germany
[b] Chemistry Department, Faculty of Science, Kafrelsheikh University,
Kafrelsheikh, Egypt
Supporting information for this article is available on the WWW under http://dx.doi.org/10.1002/ejic.200900807.

ments on the binding of NO. At present no mechanistic studies on such NO binding reactions have been performed on Fe^{II} sulfur-ligated complexes that have model character for biologically important enzymes. In principle, the reversible binding of NO to the $[Fe^{II}(S_4NR)]$ complex can be considered as a model for reversible NO binding in sulfur coordinated metal centers of nitrogenase.

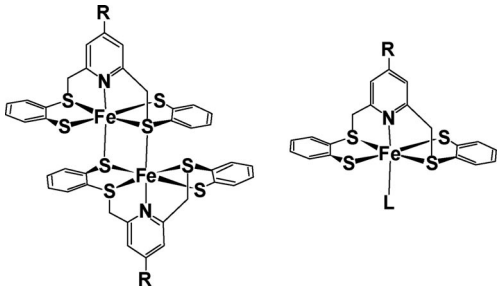

Scheme 1. Schematic presentation of di- and mononuclear iron complexes containing the $[Fe^{II}(S_4NR)]$ fragment; R = H or Et_2N; L = NO, NO^+ or CO.

Results and Discussion

Iron sulfur complexes of the formula $[Fe^{II}(S_4NNEt_2)]_2$ (**1**) have previously been shown[9a] to exist as binuclear iron clusters in which the two iron centers are connected via bis(μ-thiolato) bridges. The S_4NNEt_2 ligand acts as a square-pyramidal coordination cap and the overall geometry around the iron center is pseudo-octahedral. The pyridine N1 donor and the bridging S-donor of a second Fe fragment, as well as the two thiolate and the two thioether donors of the S_4NNEt_2 ligand, occupy pair-wise *trans*-positions. The reactions of $[Fe^{II}(S_4NNEt_2)]_2$ (**1**) with NO, NO^+ or CO gave mononuclear $[Fe^{II}(NO)(S_4NNEt_2)]$ (**3**), $[Fe^{II}(NO)(S_4NNEt_2)]^+$ (**4**) and $[Fe^{II}(CO)(S_4NNEt_2)]$ (**5**) complexes, respectively.

As for other complexes with this type of ligand, the spin state of the iron(II) sulfur complexes depends on coordination at the sixth axial position. Whereas the dinuclear complex $[Fe^{II}(S_4NNEt_2)]_2$ (**1**) is high-spin [μ_{eff} (293 K) = 5.15 μ_B], binding of a sixth ligand like NO or NO^+ produces the corresponding low-spin species. The complex $[Fe^{II}(NO)(S_4NNEt_2)]$ (**3**) was synthesized from $[Fe^{II}(S_4NNEt_2)]_2$ (**1**) by treating with a stoichiometric amount of NO. The reaction product is $[Fe^{II}(NO)(S_4NNEt_2)]$ (**3**), i.e. $\{Fe\text{-}NO\}^7$, which can formally exist as either $[Fe^{I}(NO^+)(S_4NNEt_2)]$ or $[Fe^{II}(NO^{\cdot})(S_4NNEt_2)]$. The latter form is in excellent agreement with the observation that one electron oxidation of $\{Fe\text{-}NO\}^7$ to $\{Fe\text{-}NO\}^6$ increases the NO stretching frequency from 1640 to 1884 cm^{-1} as shown in Figure 1.

The complex $[Fe^{II}(NO^{\cdot})(S_4NNEt_2)]$ (**3**) contains low-spin d^6 ferrous ion according to the zero-field Mössbauer spectra at 77 K; there is a doublet with an isomer shift, δ = 0.38(1) mm s^{-1} and quadrupole splitting ΔE_Q = 0.44(1) mm s^{-1} (see Figure 2). These parameters are close to the Mössbauer characteristics of closely related low-spin ferrous nitrosyl $[Fe^{II}(NO^{\cdot})(S_4N)]$ complexes reported by Wieghardt et al. which have an isomer shift, δ = 0.33(1) mm s^{-1} and quadrupole splitting ΔE_Q = –0.40(1) mm s^{-1}.[10] The slight isomer shift difference between $[Fe^{II}(NO^{\cdot})(S_4NNEt_2)]$ (**3**) and the related complex reported by Wieghardt et al. could be traced to the change in electron density caused by the ligand derivatives.

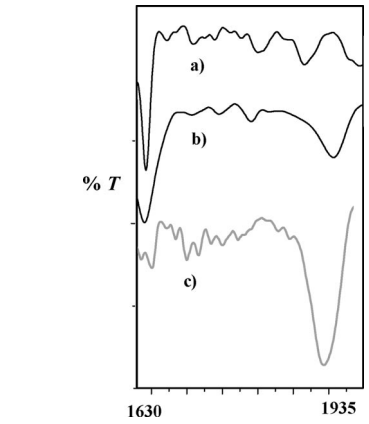

Figure 1. IR spectra (in CH_2Cl_2) of a) $[Fe^{II}(NO^{\cdot})(S_4NNEt_2)]$ (**3**); b) during the oxidation reaction; c) at the end of the reaction.

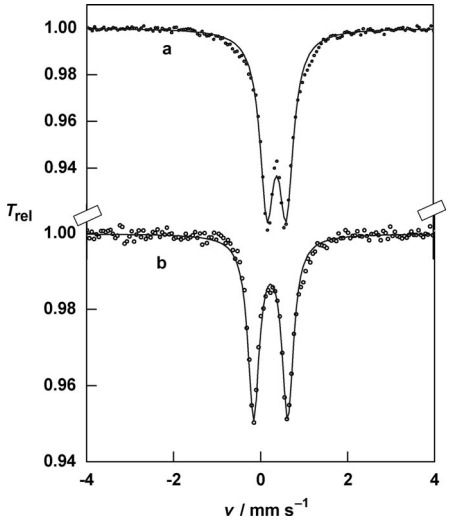

Figure 2. Zero-field Mössbauer spectra at 77 K of a) $[Fe^{II}(NO^{\cdot})(S_4NNEt_2)]$ (**3**) and b) $[Fe^{II}(CO)(S_4NNEt_2)]$ (**5**).

To test this hypothesis experimentally, we have determined the isomer shift, δ = 0.23(1) mm s^{-1}, and quadrupole splitting, ΔE_Q = 0.78(1) mm s^{-1}, from the Mössbauer spectrum of $[Fe^{II}(CO)(S_4NNEt_2)]$ (**5**). The zero-field Mössbauer spectrum clearly displays a doublet (see Figure 2). As expected, on decreasing the electron density at the metal center the isomer shift decreases to δ = 0.19(1) mm s^{-1} in $[Fe^{II}(CO)(S_4NNEt_2)]$, and at the same time, the quadrupole splitting parameter, ΔE_Q, increases to 0.88(1) mm s^{-1}.[11] Thus, based on the IR and Mössbauer spectroscopic data, the iron nitrosyl complex $[Fe^{II}(NO^{\cdot})(S_4NNEt_2)]$ (**3**) is a six-coordinate, low-spin Fe^{II} complex with a neutral NO li-

gand. This nitric oxide ligand adopts an interjacent bent geometry and its electronic structure is best described as a delocalized $\{Fe^{II}\text{-}NO^{\cdot}\}^7$ configuration.[11]

Kinetic Studies of the Binding of NO to [Fe(S_4N*Et*$_2$*N*)] Fragments

The complex $[Fe^{II}(S_4N\mathit{NEt_2})]_2$ has also been shown to exist in both mono- and dinuclear forms in solution, i.e. **2** and **1**, respectively, with the latter being favored at low and room temperature. When no additional nucleophile is present, two mononuclear complexes (**2**) fold together to form the dinuclear complex (**1**). In order to bind the nucleophile, the bridge unfolds and allows a relatively open access to the active site. Evidence for the dinuclear species in solution comes from its very low solubility as well as the mass spectrum which shows a molecular ion peak at m/z = 1024 that corresponds to the dinuclear species (**1**). NO binding to the dinuclear complex $[Fe^{II}(S_4N\mathit{NEt_2})]_2$ was kinetically investigated and occurs according to the overall reaction (1).

$$[Fe^{II}(S_4N\mathit{NEt_2})]_2 + 2NO \rightarrow 2[Fe^{II}(NO^{\cdot})(S_4N\mathit{NEt_2})] \quad (1)$$

Reaction (1) can be monitored spectrophotometrically over the wavelength range 300 to 375 nm. Solutions were prepared by dissolving known amounts of complex **1** in methanol and used directly after dissolution. The NO binding reactions were studied as a function of NO concentration, temperature and pressure in methanol. A representative kinetic trace recorded during the binding of NO to $[Fe^{II}(S_4N\mathit{NEt_2})]_2$ (**1**) is shown in Figure 3. Rate constants for the reaction were determined by using total NO concentrations in the range of 1.0–7.0 mM, i.e. always at least a 10-fold excess over the Fe^{II} complex concentration. Throughout the NO concentration range it was possible to fit the absorbance/time traces to single-exponential function as shown in Figure 3. It follows that k_{obs} should depend linearly on the entering NO concentration in the absence of a back reaction as shown in Figure 4, such that $k_{obs} = k_2$[NO] which leads to the second-order rate constant k_2 = 2400 ± 100 $M^{-1}s^{-1}$.

The reaction of $[Fe^{II}(S_4N\mathit{NEt_2})]_2$ (**1**) with NO was studied as a function of temperature in the range from 10 to 30 °C and the observed temperature dependence is reported in Figure 5. The plot is linear over the temperature range studied and $\Delta H^{\#}$ and $\Delta S^{\#}$ have the values 31 ± 1 kJ mol^{-1} and –81 ± 4 J K^{-1} mol^{-1}, respectively. The effect of pressure on the binding of NO was studied by stopped-flow technique in the range from 10 to 130 MPa. A NO concentration of 1.5 mM was selected to study the pressure dependence of k_{obs} for the binding of NO. The reaction rate increases drastically with increasing pressure, even for the lowest accessible NO concentration selected for the experiments. The plot of lnk_{obs} vs. pressure is linear as shown in Figure 6. The value of the activation volume $\Delta V^{\#}$ = –21 ± 1 cm^3 mol^{-1} was obtained from the slope of the plot according to the equation:

$$\Delta V^{\#} = -RT(\delta \ln k/\delta P)_T$$

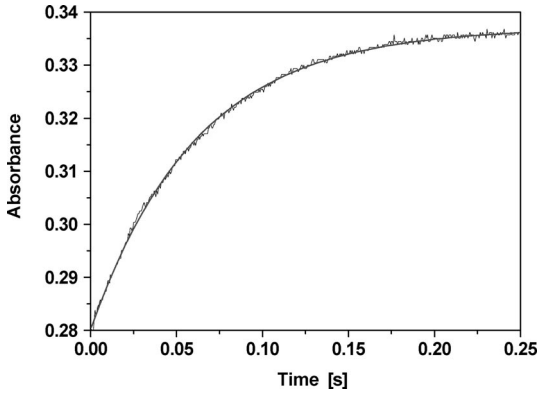

Figure 3. Representative kinetic trace for the reaction between the dinuclear complex $[Fe^{II}(S_4N\mathit{NEt_2})]_2$ (**1**) and NO in methanol obtained by stopped-flow spectrophotometry (solid line was obtained by fitting the data with a single exponential function). Experimental conditions: T = 296 K. [**1**] = 0.5 × 10^{-4} M, [NO] = 7 mM, λ = 351 nm.

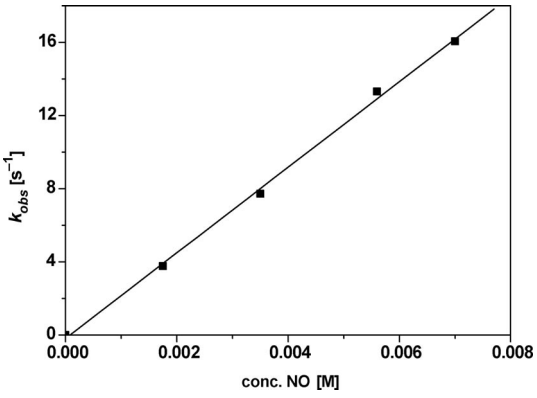

Figure 4. Plot of k_{obs} vs. NO concentration for the dinuclear complex $[Fe^{I}(^{I}S_4N\mathit{NEt_2})]_2$ (**1**) in MeOH at 296 K, [**1**] = 0.5 × 10^{-4} M, λ = 351 nm.

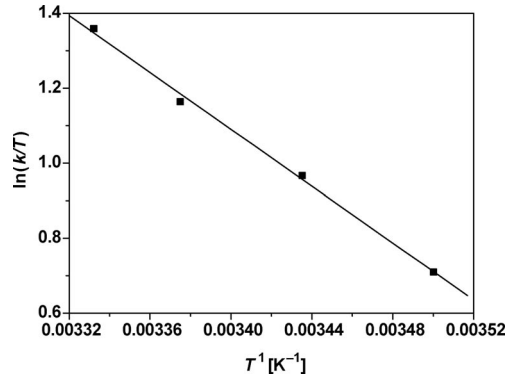

Figure 5. Temperature dependence of the reaction of the dinuclear $[Fe^{II}(S_4N\mathit{NEt_2})]_2$ complex (**1**) with NO in MeOH. Experimental conditions: [**1**] = 0.5 × 10^{-4} M, [NO] = 3.5 mM, λ = 351 nm.

In general, bond formation is expected to show a negative volume of activation as a result of an intrinsic volume collapse.[12] The quantitative interpretation of $\Delta V^{\#}$ for reaction (1) can include several contributions, such as the intrinsic volume collapse due to an overlap of van der Waals

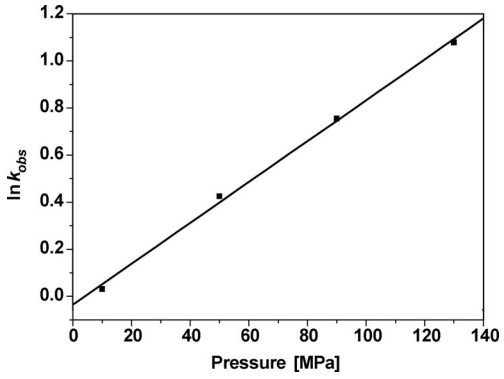

Figure 6. Pressure dependence of the reaction of complex **1** with NO in methanol. Experimental conditions: [**1**] = 0.5×10^{-4} M, [NO] = 1.5 mM, 296 K, λ = 351 nm.

spheres during the bond-formation process, and contributions that arise from a spin change on the ferrous center, i.e., quintet to singlet transition (negative contribution), and desolvation of the coordinating ligand (positive contribution). The association process is also characterized by a significantly negative activation entropy, $\Delta S^{\#} = -81 \pm 4\ J\,K^{-1}\,mol^{-1}$ (Figure 5, Table 1), which is consistent with the entrance of NO into the coordination sphere. Furthermore, the activation volume for the binding of NO is significantly negative, viz. $\Delta V^{\#} = -21 \pm 1\ cm^3\,mol^{-1}$. Substantially positive contributions to $\Delta S^{\#}$ and $\Delta V^{\#}$ resulting from the desolvation processes are not expected, since as it has been established before that the iron(II) complex exists in methanol and dichloromethane solution as six-coordinate species, with the sixth coordination site in the axial position occupied by the thiolato bridge.[9a] Several studies have been reported on various iron(II) complexes that exist in high-spin/low-spin electronic state equilibria,[10,13–17] and these have shown that the volume changes associated with such a spin transition of d^6 iron(II) fall in the range from –4 to –22 $cm^3\,mol^{-1}$, depending on the solvent and ligand structure around the metal.[13–15] The volume of activation found for the binding of NO in the present study lies within this range of values and supports that Fe–NO bond formation can involve a contribution from the high-spin to low-spin transition.

Table 1. Rate and activation parameters for the binding of NO to the dinuclear $[Fe^{II}(S_4NNEt_2)]_2$ (**1**), mononuclear $[Fe^{II}(CH_3OH)(S_4NNEt_2)]$ (**2**) and $[Fe^{II}(CO)(S_4NNEt_2)]$ (**5**) complexes at 296 K.

Complex	k_2 [$M^{-1}\,s^{-1}$]	$\Delta H^{\#}$ [$kJ\,mol^{-1}$]	$\Delta S^{\#}$ [$J\,K^{-1}\,mol^{-1}$]	$\Delta V^{\#}$ [$cm^3\,mol^{-1}$]
1[a]	2400 ± 100	31 ± 1	–81 ± 4	–21 ± 1
2[a]	17500 ± 300	35 ± 1	–47 ± 5	–
5[b]	2620 ± 160	12.5 ± 0.7	–133 ± 2	–6.7 ± 0.3

[a] Solvent is methanol. [b] Solvent is toluene.

Because complex **1** exists mostly as the six-coordinate species even at room temperature, the binding of NO to this complex involves the reaction of NO with a coordinately saturated complex instead of a five-coordinate iron(II) species. Presumably, the mechanism involves a pre-equilibrium between the predominant di- and mononuclear species. Therefore, when complex **1** was stirred for a long time (ca. 6 h) or placed in an ultrasonic bath for about 30 min in a coordinating solvent like methanol, the pre-equilibrium between di- and mononuclear species shifted to the mononuclear species. This could be seen in the mass spectrum as a molecular ion peak at m/z = 552 (100%) corresponding to the mononuclear species was formed. Furthermore, the UV/Vis spectrum changed during stirring in methanol (see Figure 7). The mononuclear species was expected to be either a five-coordinate species with a vacant coordination site or a six-coordinate species with methanol coordinated in the sixth coordination site. The possible formation of a five-coordinate species could be eliminated because the dissociation could only be seen in coordinating solvents like methanol, and not in a non-coordinating solvent like toluene (Figure 7).

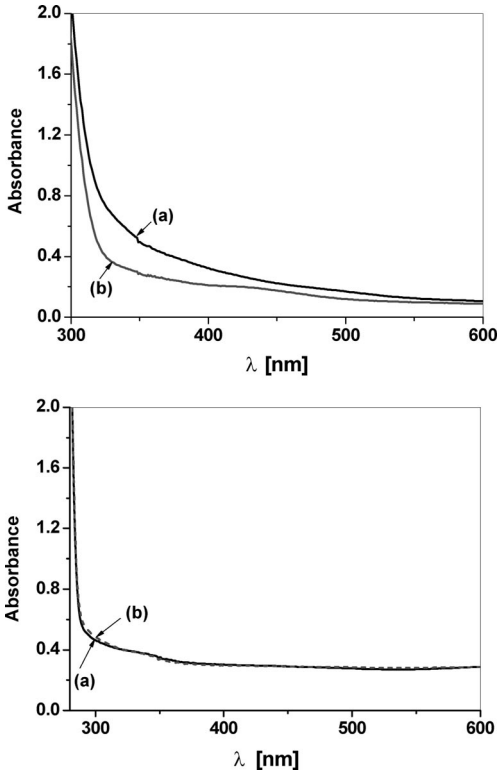

Figure 7. UV/Vis spectral changes recorded for complex **1** (0.5×10^{-4} M) in MeOH (top) and in toluene (bottom) at 296 K: (a) as obtained directly after dissolution; (b) as obtained after 6 h of stirring.

The kinetic behavior of the mononuclear complex with NO was also investigated in methanol in order to correlate the results with those for the dinuclear complex. A representative kinetic trace for this reaction is shown in Figure 8, and the plot of k_{obs} vs. NO concentration is shown in Figure 9. The reaction was studied as a function of temperature in the limited range from 4 to 23 °C due to the relatively high rate of the process, and the activation enthalpy and entropy were estimated (see Figure S1 in Supporting

Information and Table 1). The rate constant and the activation parameters for the reaction of NO with the mononuclear complex **2** are $k = 17500 \pm 300\ M^{-1}s^{-1}$, $\Delta H^{\#} = 35 \pm 1\ kJ\,mol^{-1}$ and $\Delta S^{\#} = -47 \pm 2\ J\,K^{-1}\,mol^{-1}$. It follows that complex **2** reacts approx. 7 times faster with NO than complex **1**. The effect of pressure on k_{obs} could not be studied due to the high rate of this reaction. On comparing the activation parameters of the reaction of both di- and mononuclear complexes with NO, we find that both reactions show very negative $\Delta S^{\#}$ values of -81 ± 4 and $-47 \pm 2\ J\,K^{-1}\,mol^{-1}$, respectively, which clearly indicate that the reaction with NO follows an associative mechanism. Further support for an associative mechanism is the significantly negative volume of activation for the reaction of NO with the dinuclear species ($\Delta V^{\#} = -21 \pm 1\ cm^3\,mol^{-1}$). The reaction with the dinuclear complex is 8 times slower than with the mononuclear species. This means that the observed rate constant for the binding of NO to the dinuclear complex must involve a contribution from bond cleavage to form the mononuclear complex.

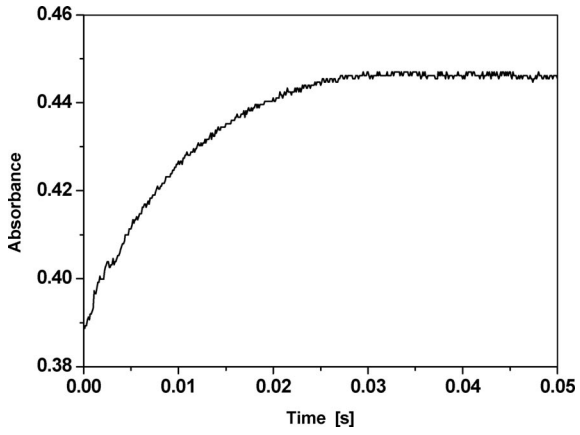

Figure 8. Representative kinetic trace recorded at 351 nm for the reaction between the mononuclear complex [$Fe^{II}(CH_3OH)(S_4NNEt_2)$] (**2**) and NO in MeOH obtained by stopped-flow spectrophotometry. Experimental conditions: $T = 296$ K, [**2**] = 0.5×10^{-4} M, [NO] = 7 mM.

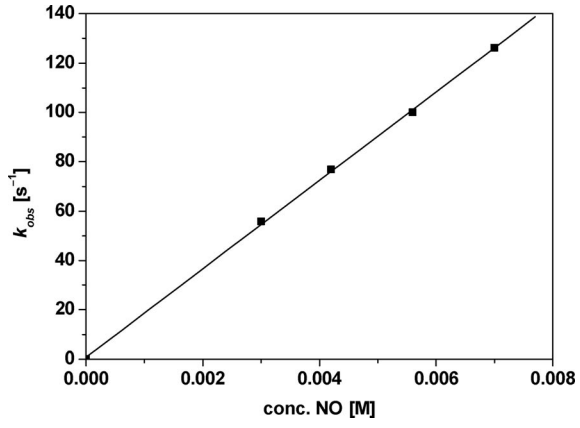

Figure 9. Plot of k_{obs} vs. NO concentration for the mononuclear complex [$Fe^{II}(CH_3OH)(S_4NNEt_2)$] (**2**) in MeOH at 296 K, [**2**] = 0.5×10^{-4} M, $\lambda = 351$ nm.

The difference in reactivity of both complexes can therefore be understood in terms of: 1) the bond strength of the leaving coligand, i.e. the stronger the metal–coligand bond, the slower the reaction rate, and in this case the metal–methanol bond is weaker than the metal–thiolate bond. 2) It is known that free heme model compounds usually show faster association and dissociation rates than found in hemeproteins as a result of the steric hindrance[1] and in this case the steric hindrance around the iron complex is higher in the case of the dinuclear complex as compared to the mononuclear species, which will slow down the associative binding of NO. Taking into account all the above information, the mechanism for the reaction of NO with dimer **1** can be represented as shown in Scheme 2. The addition of NO to the dimer followed by cleavage of the Fe–S–Fe bridges to form a NO complex and a monomer **2**, appears to be the rate-determining step of the overall reaction. The second step in which NO reacts with the monomer **2** is significantly faster (Scheme 2), as evidenced by the kinetic data reported for this reaction above.

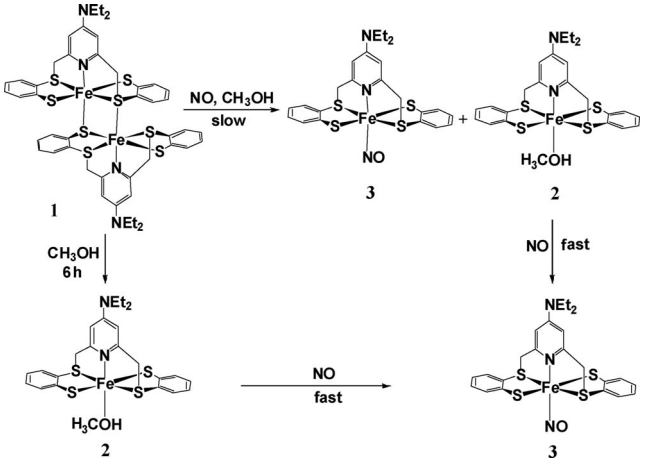

Scheme 2. Suggested mechanism for the reaction of NO with the dimer **1** and the monomer **2**.

Binding of NO to [$Fe^{II}(CO)(S_4NEt_2N)$]

In order to further investigate the suggested mechanism outlined in Scheme 2, the reaction of NO with the mononuclear complex [$Fe^{II}(CO)(S_4NEt_2N)$] (**5**) in which the sixth coordination site is occupied by CO was also investigated. The [$Fe^{II}(CO)(S_4NEt_2N)$] (**5**) complex can be prepared through the coordination of CO to both complexes **1** or **2**.[9a] Complex **5** can undergo a ligand-substitution reaction with NO to form complex **3** as shown in Scheme 3.

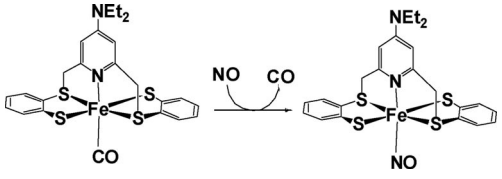

Scheme 3. Schematic representation of the reaction of complex **5** with NO to form complex **3**.

This reaction is accompanied by a significant absorbance decrease around 325 nm and can be studied using stopped-flow techniques (see Figure 10). The results for the dependence of the observed first-order rate constant on the concentration of NO are presented in Figure S2 (see Supporting Information), from which it follows that the reaction in Scheme 3 has a first-order dependence on the concentration of NO with no significant intercept, i.e. no apparent back reaction. The temperature and pressure dependence of this reaction were studied (see Figure 11 and S3, Supporting Information), and the rate and activation parameters are included in Table 1. The reported rate constant is very similar to that found for the dinuclear complex **1**, which is due to the high stability of both complexes **1** and **5**.

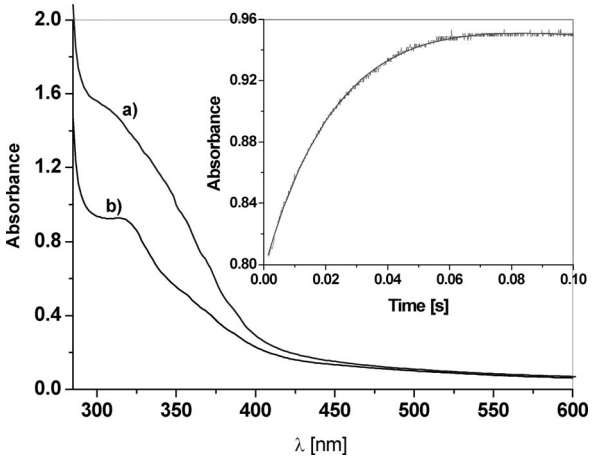

Figure 10. UV/Vis spectra recorded for the reaction of complex **5** (0.5×10^{-4} M) with NO (5.5 mM) in toluene at 296 K: (a) as observed before the reaction; (b) as obtained after 0.1 s at the end of the reaction. Inset shows kinetic trace recorded under the same conditions at 336 nm (solid line was obtained by fitting the data with a single exponential function).

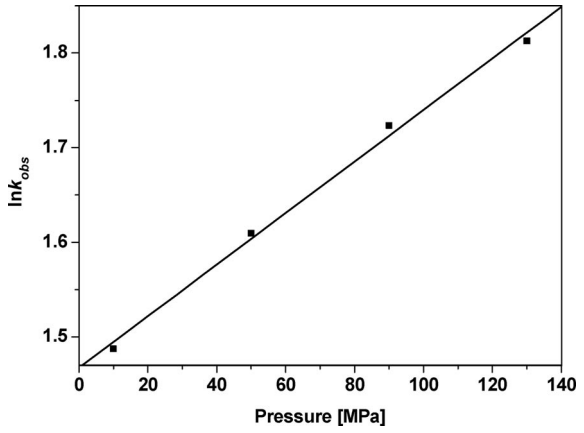

Figure 11. Plot of lnk_{obs} vs. pressure for the reaction of [Fe(CO)(Et_2NpyS$_4$)] (**5**) with NO in toluene followed at 336 nm. Experimental conditions: [**5**] = 0.5×10^{-4} M, [NO] = 1.5 mM at 296 K.

The activation entropy and activation volume data clearly support the operation of an associative substitution reaction and once again are in line with the data reported for complex **1**. The volume of activation for the reaction of complex **1** with NO is much more negative than that for the reaction of complex **5** according to the data in Table 1. As mentioned above, in the case of complex **1** the very negative volume of activation was ascribed to contributions from the binding of NO and a high-spin to low-spin changeover. In the case of complex **5** the binding of NO does not involve a change in spin state, which accounts for the less negative activation volume found for this reaction.

Conclusions

In conclusion, structural and mechanistic information on the binding of NO to the di- and mononuclear complexes **1** and **2** as potential catalysts for the removal of NO from gaseous effluents have been obtained from the relative reaction rates, temperature and pressure dependence studied by using stopped-flow techniques. The results further indicate that steric and electronic parameters affect the rate but not the nature of the substitution mechanism by which NO coordinates to the selected complexes. Therefore, the sterically hindered dinuclear [Fe^{II}(S$_4$NNEt_2)]$_2$ complex binds NO significantly slower than the corresponding mononuclear [Fe^{II}(CH_3OH)(S$_4$NNEt_2)] complex. A similar finding is true for the carbonyl complex **5** in which the stability of the Fe–CO bond accounts for the slow ligand displacement reaction. Large and negative $\Delta S^{\#}$ values were found for the binding of NO to complexes **1**, **2** and **5**, consistent with an associative mechanism. The large and negative volumes of activation observed for the binding of NO to complexes **1** and **5** further underlines the operation of an associative binding mechanism.

In the case of complex **1**, the high- to low-spin transition of the iron center is suggested to contribute to the more negative activation volume as compared to complex **5**. A comparison of the [Fe^{II}(S$_4$NNEt_2)] complexes with heme proteins in the ferrous state in terms of their electronic structure, binding to NO as well as stability, reveals that: i) [Fe^{II}(S$_4$NNEt_2)] complexes and the ferrous heme bind strongly[18] to NO as a neutral ligand; ii) [Fe^{II}(NO)(S$_4$NNEt_2)] and the ferrous nitrosyl heme are stable complexes with low dissociation rates,[19] as preliminary results showed that the [Fe^{II}(NO)(S$_4$NNEt_2)] complex releases NO very slowly in solution and such a feature is of importance for efficient NO transport; iii) NO activates sGC by binding to the ferrous iron in the heme pocket ($k_{on} > 10^5$ M^{-1} s^{-1})[20] which is faster than that of [Fe^{II}(S$_4$NNEt_2)] complexes. [Fe^{II}(S$_4$NNEt_2)] complexes were found to bind NO much slower than non-heme complexes containing the ferrous iron, such as [Fe^{II}(H_2O)$_6$]$^{2+}$ (1.4×10^6 M^{-1} s^{-1} at 25 °C)[21] and [Fe^{II}(EDTA)H_2O] (2.4×10^8 M^{-1} s^{-1} at 25 °C).[22] Studies on the [Fe^{II}(NO)(S$_4$NNEt_2)] complex as NO delivery agent are now in progress.

Experimental Section

Materials: [Fe(S$_4$NNEt_2)]$_2$ (**1**), [Fe(NO$^{\cdot}$)(S$_4$NNEt_2)] (**3**), [Fe(NO$^+$)(S$_4$NNEt_2)]BF_4 (**4**) and [Fe(CO)(S$_4$NNEt_2)] (**5**) were synthesized as

described in the literature.[9a] All chemicals used in this work were of analytical grade or better. Solvents were degassed prior to use and kept under nitrogen. Solutions of the complexes were all freshly prepared under nitrogen atmosphere prior to the kinetic and equilibrium studies. The concentration of the complex was usually in the range of 5×10^{-5} M, and measurements were performed in methanol. For the dinuclear complex **1** and complex **5**, the measurements were performed directly after dissolution in methanol, whereas for the mononuclear complex **2**, the measurements were performed after about 6 h of stirring in methanol.

Instrumentation and Measurements: Spectra were recorded on the following instruments: IR (KBr discs, solvent bands were compensated): Mattson Infinity instrument (60 AR) at 4 cm^{-1} resolution in the 400–4000 cm^{-1} range; NMR: Jeol-JNM-GX 270, EX 270, and Lambda LA 400 with the protio-solvent signal used as an internal reference. Mass spectra: Jeol MSTATION 700 spectrometer; elemental analyses: Carlo–Erba EA 1106 or 1108 analyzer. ^{57}Fe Mößbauer spectra were recorded on a WissEl Mößbauer spectrometer (MRG-500) at 77 K in the constant acceleration mode. ^{57}Co/Rh was used as the radiation source. WinNormos for Igor Pro software was used for the quantitative evaluation of the spectral parameters (least-squares fitting to Lorentzian peaks). The minimum experimental line widths were 0.21 mm s^{-1}. The temperature of the samples was controlled by an MBBC-HE0106 MÖSSBAUER He/N_2 cryostat within an accuracy of ± 0.3 K. Isomer shifts were determined relative to α-iron at 298 K.

Kinetic investigations were performed either in tandem cuvettes with a path length of 0.88 cm, thermally equilibrated at 23.0 ± 0.1 °C before mixing, using a Varian Cary 1G spectrophotometer, or on an Applied Photophysics SX 18MV stopped-flow instrument with an optical path length of 1 cm at 351 nm. For experiments at elevated pressure (1–130 MPa), a laboratory-made high-pressure stopped-flow instrument was used.[23] The temperature of the instruments was thermostatted at 23.0 ± 0.1 °C. The solubility of NO was taken to be 14 mM in methanol and 11 mM in toluene at 23 °C. NO solutions of known composition were generated using a Tylan TO-28 controller with model FC-260 mass flow controllers and compressed gas cylinders of the pure gas. The ligand-substitution reactions were studied under pseudo-first-order conditions by using at least a ten-fold excess of NO. All listed rate constants represent an average value of at least three kinetic runs under each experimental condition.

Supporting Information (see also the footnote on the first page of this article): Temperature dependence of the reactions of the mononuclear complex **2** with NO in MeOH and of **5** with NO in toluene. Plot of k_{obsd} vs. NO concentration for the reaction with **5** in toluene.

Acknowledgments

The authors gratefully acknowledge financial support from the Deutsche Forschungsgemeinschaft (DFG) and the Egyptian Ministry of Higher Education and Scientific Research.

[1] a) V. Zang, R. van Eldik, *Inorg. Chem.* **1990**, *29*, 4462–4468; b) E. K. Pham, S. G. Chang, *Nature* **1994**, *369*, 139–141; c) J. A. McCleverty, *Chem. Rev.* **2004**, *104*, 403–418.

[2] a) S. Moncada, R. M. J. Palmer, E. A. Higgs, *Pharmacol. Rev.* **1991**, *43*, 109–142; b) M. Feelish, J. S. Stamler, in: *Methods in Nitric Oxide Research* (Eds.: M. Feelish, J. S. Stamler), Wiley, New York, **1996**, pp. 3–45; c) P. L. Feldman, O. W. Griffith, D. J. Stuehr, *Chem. Eng. News* **1993**, *71*, 26–31; d) A. R. Butler, D. L. H. Williams, *Chem. Soc. Rev.* **1993**, *22*, 223–241; e) D. E. Koshland, *Science* **1992**, *258*, 1861–1861; f) R. M. J. Palmer, A. G. Ferrige, S. Moncada, *Nature* **1987**, *327*, 524–526; g) F. Murad, *Angew. Chem.* **1999**, *111*, 1976–1989; *Angew. Chem. Int. Ed.* **1999**, *38*, 1856–1868; h) P. G. Wang, T. B. Cai, N. Taniguchi (Eds.), *Nitric Oxide Donors*, Wiley-VCH, Weinheim, Germany, **2005**; i) S. A. T. Dillinger, H. W. Schmalle, T. Fox, H. Berke, *Dalton Trans.* **2007**, 3562–3571.

[3] T. Noguchi, J. Honda, T. Nagamune, H. Sasabe, Y. Inoue, I. Endo, *FEBS Lett.* **1995**, *358*, 9–12.

[4] M. W. J. Cleeter, J. M. Cooper, V. M. Darley-Usmar, S. Moncada, A. H. V. Scapira, *FEBS Lett.* **1994**, *345*, 50–54.

[5] a) J. B. Howard, D. C. Rees, *Chem. Rev.* **1996**, *96*, 2965–2982; b) B. K. Burgess, D. J. Lowe, *Chem. Rev.* **1996**, *96*, 2983–3012; c) R. R. Eady, *Chem. Rev.* **1996**, *96*, 3013–3030.

[6] a) M. J. Clarke, J. B. Gaul, *Struct. Bonding (Berlin)* **1993**, *81*, 147–181; b) B. Serli, E. Zangrando, T. Gianferrara, L. Yellowlees, E. Alessio, *Coord. Chem. Rev.* **2003**, *245*, 73–83; c) A. K. Patra, P. K. Mascharak, *Inorg. Chem.* **2003**, *42*, 7363–7365; d) E. Tfouni, M. Krieger, B. R. McGarvey, D. W. Franco, *Coord. Chem. Rev.* **2003**, *236*, 57–69; e) M. J. Clarke, *Coord. Chem. Rev.* **2002**, *232*, 69–93.

[7] a) P. Legzdins, C. C. Y. Pang, M. J. Shaw, Compositions and Methods for Relaxing Smooth Muscles. U. S. Patent 5,631,284, May 20, **1997**; b) P. Legzdins, C. C. Y. Pang, M. J. Shaw, *Compositions and Methods for Relaxing Smooth Muscles*, U. S. Patent 5,811,463, September 22, **1998**; c) B. A. Averill, *Chem. Rev.* **1996**, *96*, 2951–2964.

[8] a) M. Hoshino, L. Laverman, P. Ford, *Coord. Chem. Rev.* **1999**, *187*, 75–102; b) M. Wolak, R. van Eldik, *Coord. Chem. Rev.* **2002**, *230*, 263–282.

[9] a) D. Sellmann, S. Y. Shaban, F. W. Heinemann, *Eur. J. Inorg. Chem.* **2004**, *23*, 4591–4601; b) D. Sellmann, N. Blum, F. W. Heinemann, B. A. Hess, *Chem. Eur. J.* **2001**, *7*, 1974–1980; c) D. Sellmann, N. Blum, F. W. Heinemann, *Z. Naturforsch., Teil B: Chem. Sci.* **2001**, *56*, 581–588.

[10] M. Li, D. Bonnet, E. Bill, F. Neese, T. Weyhermller, N. Blum, D. Sellmann, K. Wieghardt, *Inorg. Chem.* **2002**, *41*, 3444–3456.

[11] A. I. Poddel'sky, M. P. Bubnov, G. K. Fukin, V. K. Cherkasov, G. A. Abakumov, *Z. Anorg. Allg. Chem.* **2008**, *634*, 1205–1209.

[12] R. van Eldik, H. Kelm, *Rev. Phys. Chem. Jpn.* **1980**, *50*, 185–206.

[13] J. DiBenedetto, V. Arkle, H. A. Goodwin, P. C. Ford, *Inorg. Chem.* **1985**, *24*, 456–459; D. Sellmann, J. Sutter, *Prog. Inorg. Chem.* **2003**, *52*, 585–681; K. H. Hopmann, A. Ghosh, L. Noodleman, *Inorg. Chem.* **2009**, *48*, 9155–9165.

[14] J. J. McGarvey, I. Lawthers, K. Heremans, H. Toflund, *J. Chem. Soc., Chem. Commun.* **1984**, 1575–1576.

[15] J. K. Beattie, R. A. Binstead, R. J. West, *J. Am. Chem. Soc.* **1978**, *100*, 3044–3050.

[16] R. A. Binstead, J. K. Beattie, T. G. Dewey, D. H. Turner, *J. Am. Chem. Soc.* **1980**, *102*, 6442–6451.

[17] M. Buchalova, D. H. Busch, R. van Eldik, *Inorg. Chem.* **1998**, *37*, 1116–1120.

[18] a) G, S. J. R. Deinum, G. T. Babcock, M. A. Marletta, *Biochemistry* **1996**, *35*, 1540–1547; b) A. Tsai, *FEBS Lett.* **1994**, *341*, 141–145.

[19] a) G. Deinum, J. R. Stone, G. T. Babcock, M. A. Marletta, *Biochemistry* **1996**, *35*, 1540–1547; b) R. Hille, J. S. Olson, G. Palmer, *J. Biol. Chem.* **1979**, *254*, 12110–12116; c) V. S. Sharma, H. M. Ranney, *J. Biol. Chem.* **1978**, *253*, 6467–6472.

[20] a) J. C. Edwards, B. K. Barry, D. Y. Gruetter, E. H. Ohlstein, W. H. Baricos, L. J. Ignarro, *Biochem. Pharmacol.* **1981**, *30*, 2531–2538; b) R. Gerzer, F. Hofmann, G. Schultz, *Eur. J. Biochem.* **1981**, *116*, 479–486; c) L. J. Ignarro, J. N. Degnan, W. H. Baricos, P. J. Kadowitz, M. S. Wolin, *Biochim. Biophys. Acta* **1982**, *718*, 49–59; d) L. J. Ignarro, K. S. Wood, M. S. Wolin, *Proc. Natl. Acad. Sci. USA* **1982**, *79*, 2870–2873; e) J. R. Stone, M. A. Marletta, *Biochemistry* **1995**, *34*, 16397–16403; f) D. A.

Pixton, C. A. Petersen, A. Franke, R. van Eldik, E. M. Garton, C. R. Andrew, *J. Am. Chem. Soc.* **2009**, *131*, 4846–4859.
[21] A. Wanat, T. Schneppensieper, G. Stochel, R. van Eldik, E. Bill, K. Wieghardt, *Inorg. Chem.* **2002**, *41*, 4–10.
[22] T. Schneppensieper, A. Wanat, G. Stochel, S. Goldstein, D. Meyerstein, R. van Eldik, *Eur. J. Inorg. Chem.* **2001**, 2317–2325.
[23] R. van Eldik, W. Gaede, S. Wieland, J. Kraft, M. Spitzer, D. A. Palmer, *Rev. Sci. Instrum.* **1993**, *64*, 1355–1357.

Received: August 18, 2009
Published Online: December 17, 2009

